

THE IMPACT OF HIGH NONCONDENSIBLE GAS CONCENTRATIONS ON WELL PERFORMANCE KIZILDERE GEOTHERMAL RESERVOIR, TURKEY

Jill Robinson Haizlip¹, Aygun Guney², Fusun S. Tut Hakkıdır², and Sabodh K. Garg³

1-Geologica Inc. 5 3rd St. #224 San Francisco, CA 93105 USA
2- Zorlu Energy Group, Zorlu Plaza, Avcılar, İstanbul, 34310, TURKEY
3-SAIC 10260 Campus Point Drive, San Diego, CA 92121 USA
e-mail: jhaizlip@geologica.net

ABSTRACT

Noncondensable gas is a major factor affecting the reservoir pressure in the deep liquid-dominated Kizildere geothermal reservoir which is currently being developed by ZORLU ENDÜSTRİYEL VE ENERJİ TESİSLERİ İNŞ.TİC.A.Ş.(Zorlu Enerji) as the Kizildere II Geothermal Power Project. Under static conditions, the pressure within the production zone ranges from 130 to 230 bar at 1700 to 2500m. Reservoir temperatures range from 219 to 242°C and under static conditions, the reservoir fluid is entirely in the liquid phase. Based on gas pressures estimated from applying Henry's law, approximately 60 bar (at 0.024 kg NCG/kg reservoir brine) to 100 bar (at 0.0415 kg NCG/kg reservoir brine) is dissolved noncondensable gas pressure. The noncondensable gas is over 98% carbon dioxide. The reservoir fluids at Kizildere are known to produce calcite scale in the wellbores at the depth of gas breakout.

The gas breakout pressures (or bubble point) is the pressure below which the fluid will begin to transform from 100% liquid to two-phase. Gas breakout pressure is the sum of the gas pressure and water pressure at the reservoir temperature. These values can be estimated using Henry's Law and the steam tables. In the deep reservoir at Kizildere, bubble points are between 80 bar (at 0.024 kg NCG/kg reservoir brine) and 128 bar (at 0.0415 kg NCG/kg reservoir brine). At the flow rates (<250 tph) that the dynamic surveys are run, measured pressure in the well falls below this gas breakout pressure between 900 and 1800 m. Wellbore simulation is used to estimate the depth of gas breakout at higher flow rates. Since the gas breakout occurs at greater depths at higher flow rates, it is important to estimate the depth of gas breakout at multiple mass flow rates to manage the potential effect of scaling in the feed zone as well as the depth of scale inhibitor injection.

INTRODUCTION

In the 1960s the Turkish government agency: Mineral Research & Exploration General Directorate (MTA) with some support from the United Nations explored the fumarole area east of the village of Kizildere in Western Turkey. Geological, geochemical and geophysical investigations were performed, temperature gradient holes were drilled and in 1968, a 198 °C geothermal reservoir was discovered with the drilling of KD-1. Over the next several years, approximately 20 deep wells were completed to characterize and develop the resource. In 1984, the first geothermal power generation in Turkey began at Kizildere I with an installed capacity of 20 MW_{e, gross}.

In 2008, Zorlu Energy Group (Zorlu) acquired the Kizildere field. In the fall of 2008, Zorlu began wellfield and power plant modifications and maintenance to restore Kizildere I to capacity and resource investigations and drilling to supply a 60 MW expansion. The data used in this work were developed by Zorlu as part of the testing of wells recently drilled to supply the new plant.

The Kizildere Geothermal Reservoir is located at the eastern end of an east-west trending extensional tectonic valley known as the Büyük Menderes Graben (Şimşek, 1985). The Paleozoic Metamorphic rocks that outcrop in the horst regions north and south of the reservoir area are downthrown along a series of semi-parallel east-west trending normal faults within the graben forming the basement rock, which are overlain by Tertiary sediments and alluvium and form the main reservoir rocks. These Paleozoics include marbles, schists, quartzite, calc-schists and gneiss.

The geothermal reservoir is a fractured reservoir. These semi-parallel east-west trending normal faults parallel to the graben and that cut formations from

the Tertiary to the Palaeozoic provide potential conduits for upflowing hot water at Kizildere as well as in other geothermal reservoirs related to grabens in the Aegean Extensional Province (Ciftci and Bozkurt, 2009). This province is characterized by thin crust and high heat flow. The graben-oriented faults appear to be cut by a second set of north-south trending faults in the immediate vicinity of the Kizildere reservoir. Recent seismic activity suggests that the area is tectonically active and is extending in the north-south direction (Simsek, 2003) and therefore the faults have the potential to be open and permeable.

Deep production zones at Kizildere are primarily encountered in the brittle limestone, marl, marbles, quartzite and gneiss of the Paleozoic metamorphic rocks, as in other geothermal systems related to Aegean grabens (Tarcan et al., 2000). High clay (or mica) content in layers within the metamorphics provide impermeable caps to the upwelling geothermal fluid in the permeable reservoir zones hosted in more brittle formations. It appears that production zones occur at the intersection of fractures and brittle rocks.

There are several geothermal reservoirs located along the Menderes Graben from the western end at Ortaklar to Denizli on the east. Many of these support commercial power generation from a few MW to 47MW at Germencik. Resource temperatures range from 170°C to the highest resource temperatures of 242 °C encountered at Kizildere. At least several of these reservoirs appear to have significant concentrations of noncondensable gas, predominantly carbon dioxide.

This paper addresses the effect of high noncondensable gas on reservoir and wellfield production in the deep Kizildere reservoir. The nature and possible sources of the noncondensable gas were discussed previously (Haizlip et al., 2011).

RESERVOIR CONDITIONS

The Kizildere geothermal reservoir is a layered reservoir. The uppermost layer is in Tertiary limestone which is somewhat discontinuous. The second or intermediate layer is primarily in fractured marbles in the uppermost section of the Paleozoic. The third or deepest reservoir is in the Paleozoic metamorphics. Between the reservoirs lie impermeable zones which cap each reservoir.

With the development of Kizildere II, the intermediate reservoir will continue to provide fluid supply to Kizildere I and deep reservoir will supply Kizildere II. These reservoirs are primarily

distinguished by temperature, noncondensable gas concentration and pressure.

The temperature patterns within the reservoir are consistent with a strong separation between the reservoirs. Temperature in the intermediate reservoir ranges from 170 to 200°C. Temperatures in the deep reservoir range from 225 to 242°C. Within the reservoir zones these temperatures are relatively constant over the vertical section of the reservoir but vary laterally, producing temperature well logs with low temperature gradients within the reservoir zones and high temperature gradients within the cap rocks.

While brine chemistry between the reservoirs is almost identical, the average noncondensable gas (NCG) concentration in the deep reservoir (0.03 kg NCG/kg brine) is approximately twice the shallow reservoir (0.015 kg NCG/kg brine). Gas composition is almost the same with 98 to 99% carbon dioxide (CO₂).

One of the most distinctive characteristics of the Kizildere reservoir is the pressure distribution. At the top of the deep reservoir for example reservoir pressures are approximately 130 to 150 bar.g under static conditions. Of this pressure approximately 60-100 bars is dissolved gas pressure, depending on both temperature and gas concentration. Shut-in wellhead pressures are typically near 30 bar.g and almost all of the wells flow are artesian. This gas pressure affects the well production as discussed below.

DEPTH OF GAS BREAKOUT OR BUBBLE POINT

Estimated Gas+Water Pressure and Dynamic Pressure Surveys

Gas breakout or two-phase conditions occurs at the depth at which the gas pressure plus water pressure exceeds the total pressure (bubble point depth). P_{gas} can be estimated using Henry's Law and the minimum water pressure can be estimated using steam tables as follows:

$$P_{\text{gas}} = X_{\text{gas}} * K_{\text{H}}$$

$$P_{\text{liq}} = P_{\text{water@sat T}}$$

$$P_{\text{tot}} = P_{\text{gas}} + P_{\text{liq}}$$

where K_{H} = Henry's law constant at the reservoir temperature and X_{gas} is the mole fraction of gas in the reservoir.

Table 1: Reservoir Parameters-Two Kizildere Wells

	WELL X	WELL Y
Reservoir Temperature (°C)	219	242
Noncondensable Gas (NCG) kg/kg	0.024	0.0415
Mole Fraction NCG, Xg	0.0098	0.017
Henry's Law Constant, Kh	5968	5493
Pgas (bar)	58.6	93.4
Pliq (bar)	23.2	33.5
Ptotal (bar)	81.8	126.9
Depth of Ptotal@low flow (m)	980	1790
Low (survey) flow (tonnes per hour, tph)	200	166
Casing Depth (m)	1550	1750
Depth of major entry (m)	1740	2300

The depths of these calculated pressures under dynamic conditions are shown in Figures 1 and 2. Because most dynamic surveys occur below the maximum or production flow rate, these depths are minimum gas breakout depths. The depth of gas breakout at full production flows is obtained by wellbore simulation.

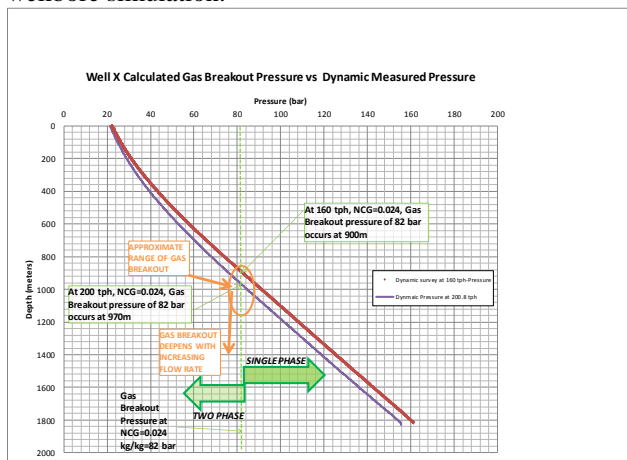


Figure 1 Gas Breakout Depth during the dynamic Survey of Well X

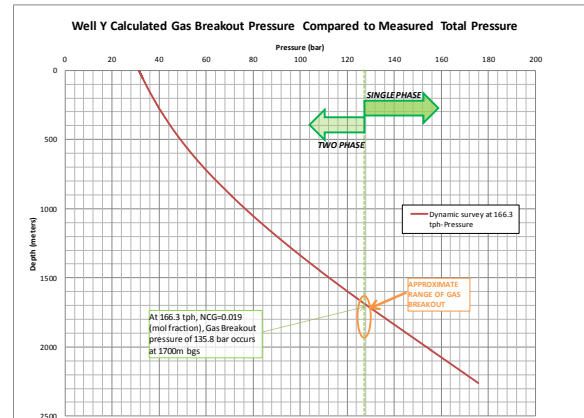


Figure 2 Gas Breakout Depth during the dynamic Survey of Well Y

Wellbore Simulation of Gas Breakout Pressure

A steady-flow wellbore model (Garg et al., 2004) was used to model the dynamic pressure and temperature profiles in wells X and Y, and thereby to constrain the values of various parameters in the wellbore model. The dynamic pressure and temperature profiles were obtained at relatively low discharge rates. The constrained wellbore models were then employed to forecast the response of the wells under various discharge rates.

Well X

A pressure, temperature and spinner (PTS) survey was run in Well X on May 7, 2011 while the well was discharging at a rate of about 200.8 tons per hour (55.8 kg/s). The spinner survey indicates that the major feedzone for the well is located at 1740 mMD (meters measured depth). The flowing feedzone pressure and temperature were 149.7 bars and 218.8 °C; the corresponding values at the wellhead were ~22.3 bars and 199 °C. Based on a pressure and temperature survey run in the shut-in well on April 21, 2011, the shut-in pressure and temperature at 1740 mMD are estimated to be 158.24 bars and ~219 °C, respectively. The productivity index (PI) for Well X is, therefore, given by:

$$PI = 55.8 / (158.24 - 149.70) = 6.534 \text{ kg/s-bar.}$$

The well geometry above the feedzone depth is summarized in Table 2.

Table 2 Well Geometry of Well X

Measured depth (m)	Vertical depth (m)	Inclination angle	Inside diameter (cm)
0-1497	0-1495.88	2.2165	22.44*
1497-1532	1495.88-1530.83	3.0630	15.71**
1532-1740	1530.83-1738.27	4.2053	21.59***

*9 5/8 inch cemented casing, ** 7 inch blank liner, ***7 inch slotted liner in 8 1/2 inch hole

Based on the static temperature survey taken on April 21, 2011, the stable formation temperature was approximated. Results are summarized in Table 3.

Table 3 Stable Formation Temperatures Well X

Measured depth (m)	Temperature (°C)
0	20
750	174
1500	215
1740	219

The reported values for reservoir fluid gas content and salinity are 0.024 kg/kg and 0.0048 kg/kg, respectively. To match the dynamic pressure profile, the gas content was adjusted slightly downwards to 0.023 kg/kg.

Except for the slotted liner, the wellbore was assumed to be smooth. A roughness of 2 mm was assumed for the slotted liner in order to match the dynamic pressure profile. The steady-state heat transfer coefficient is taken to be 4 W/m² °C. The computed values for the wellhead pressure (22.31 bars) and temperature (~202.6 °C) are in good agreement with the reported values (22.3 bars and 199 °C). The bubble point depth (depth at which a gas phase starts to form) is computed to be ~969 meters. The constrained wellbore model for Well X was then employed to investigate the response of the well to different discharge rates (Table 4).

Table 4 Well X- Simulated Bubble point depth vs Flow rates

Discharge rate (tph)	Wellhead pressure (bar)	Wellhead temperature (°C)	Bubble point depth (m)
144	23.40	202.9	935
216	21.99	202.3	978
288	20.34	200.7	1021
360	18.45	198.0	1074
432	16.16	193.6	1126
504	12.80	185.1	1178

Well Y

A pressure, temperature and spinner (PTS) survey was run in Well Y on November 30, 2011 while the well was discharging at a rate of about 166.3 tons per hour (46.2 kg/s). The spinner survey indicates that the major feedzone for the well is located at about 2300 mMD (meters measured depth). The flowing feedzone pressure and temperature were 180.73 bars and 242 °C; the corresponding values at the wellhead were ~32.4 bars and 217.9 °C. Based on a pressure and temperature survey run in the shut-in well on October 27, 2011, the shut-in pressure and temperature at 2300 mMD are estimated to be 206.48 bars and ~237 °C, respectively. The productivity index (PI) for Well Y is, therefore, given by:

$$PI = 46.2 / (206.48 - 180.73) = 1.794 \text{ kg/s-bar.}$$

The well geometry of Well Y above the feed zone is summarized in Table 5.

Table 5 Well Geometry of Well Y

Measured depth (m)	Vertical depth (m)	Inclination angle	Inside diameter (cm)
0-1701	0-1700.50	1.3893	22.44*
1701-1755	1700.50-1754.45	2.4658	15.71**
1755-2300	1754.45-2299.24	1.5906	21.59***

9 5/8 inch cemented casing, ** 7 inch blank liner, ***7 inch slotted liner in 8 1/2 inch hole

Based on the static temperature survey taken on April 21, 2011, the stable formation temperature was approximated as shown in Table 6.

Table 6 Well Y Formation Temperatures

Measured depth (m)	Temperature (°C)
0	20
650	174
2300	237

The reported values for reservoir fluid gas content and salinity are 0.0415 kg/kg and 0.0050 kg/kg, respectively. To match the dynamic pressure profile, the gas content was adjusted slightly upwards to 0.044 kg/kg. The wellbore was assumed to be

smooth. The steady-state heat transfer coefficient is taken to be 4 W/m²/°C.

The computed values for the wellhead pressure (32.16 bars) and temperature (~217.5 °C) are in good agreement with the reported values (32.4 bars and 217.9 °C). The bubble point depth (depth at which a gas phase starts to form) is computed to be ~1914 meters.

The constrained wellbore model for WELL Y was then employed to investigate the response of the well to different discharge rates. The results are given in Table 7.

Table 7 Well Y- Simulated Bubble point depth vs Flow rates

Discharge rate (tph)	Wellhead pressure (bars)	Wellhead temperature (°C)	Bubble point depth (m)
144	33.39	218.0	1880
216	29.37	215.5	2018
288	25.21	210.8	2156
360	20.48	203.3	2282

SCALING POTENTIAL IN PRODUCTION WELLS

Kizildere production fluids precipitate (scale) calcite under two-phase conditions. Observed scaling and its effect on well flows has been discussed previously (e.g. Satman et al., 1999; Arkan, et al., 2002). Calcite scaling occurs at flash points such as gas breakout (bubble) depths in Kizildere production wells (Figure 3).



Figure 3 Calcium carbonate scale accumulation at Kizildere without inhibitors

Calcite scale has been successfully mitigated by the downhole injection of phosphonate chemical carbonate scale inhibitors, which has greatly improved well performance.

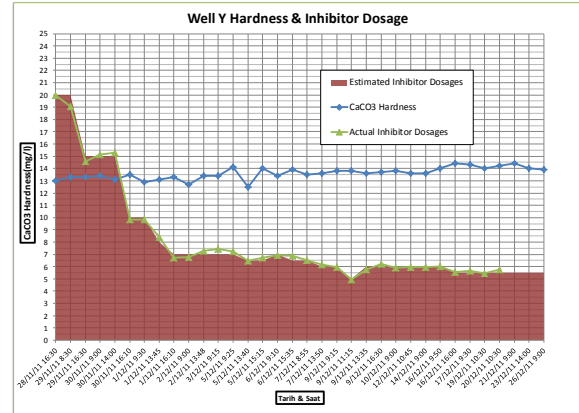


Figure 4 Calcite Scale Inhibitor Optimization Testing-Measuring Hardness (as CaCO₃) during increasing Inhibitor Dosage

Successful scale mitigation in the wellbore requires that the inhibitor is injected into the flowing well through capillary tubing at depths 10-50m below the estimated gas breakout depth preferably within the casing. If the bubble point is deeper than the casing point, then scale inhibition is more difficult as the capillary tubing must be set within the slotted liner.

Furthermore, if the gas breakout or bubble point occurs at or below the main fluid entry, calcite scale could occur in the reservoir. A comparison of the gas breakout depth versus the casing shoe and depth of the main entry (Figure 5) suggests that high (>300 tph) flow rates in wells similar to Well Y will cause in the feedzone, eventually reducing permeability and flow.

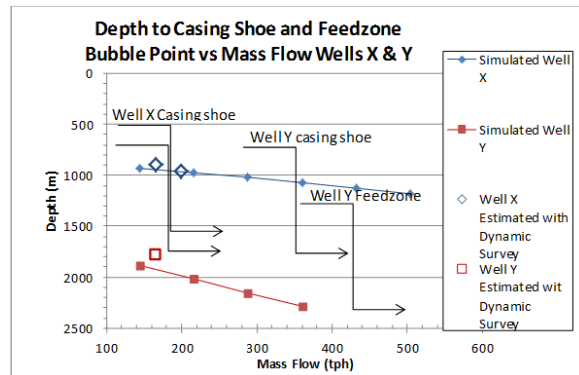


Figure 5 Increasing Bubble Point Depth with increasing Mass Flow relative to Casing Shoe and Feedzone Depths

CONCLUSIONS

The depth of gas breakout (bubble) depth in high gas wells can be estimated using the measured downhole pressures from dynamic surveys and calculated total pressure where the total pressure is equivalent to the liquid water pressure plus the gas pressure. However, this estimation is limited to the flow conditions of the dynamic survey, specifically the mass flow rate. Using wellbore simulation, the gas breakout depth can be estimated at multiple flow rates.

Results imply that for all practical discharge rates of Well X, the bubble point will remain within the cased and cemented portion of the borehole and above the main fluid entry. Therefore scale can be mitigated with practical set depth for the capillary tubing. However, results for Well Y imply that for all practical discharge rates, the bubble point is located within the slotted 7 inch liner. For a discharge rate of about 360 tph, the two-phase zone will extend to the feedzone depth, and risk of scaling the feed zone occurs. Evaluation of gas breakout or bubble points is a critical reservoir management tool for high gas liquid-dominated geothermal resources.

REFERENCES

Arkan, S., Akin, S. and Parlaktuna, M. (2002) "Effect of Calcite Scaling on Pressure Transient Analysis of Geothermal Wells", *Proceedings, 27th Workshop on Geothermal Reservoir Engineering*, Stanford University, Stanford, California, January 28-30, 2002, SGP-TR-171.

Garg, S.K., Pritchett, J.W., Alexander, J.H. (2004). A new liquid hold-up correlation for geothermal wells. *Geothermics* 33, 795-817.

Haizlip, J. R., Tut, F. (2011) High Noncondensable Gas Liquid Dominated Geothermal Reservoir Kizildere, Turkey, Geothermal Resources Council *Transactions*, Vol. 35, October 23-26, 2011.

Satman A., Ugur Z., and Onur M., (1999), "The Effect of Calcite Deposition on Geothermal Well Inflow Performance," *Geothermics*, 28, 425-444. *Journal of Fluid Mechanics*, **254**, 73-79.